

TIME-DEPENDENT CALCULATION METHOD FOR

## TRANSONIC NOZZLE FLOWS

P. Laval

Translation of: "Méthode Instationnaire  
de Calcul de L'écoulement Transsonique  
dans une Tuyère", Office National d'Etudes  
et de Recherches Aérospatiales, Chatillon,  
France, ONERA Technical Note, No. 173,  
1970, 28 pages.

Reproduced by  
**NATIONAL TECHNICAL  
INFORMATION SERVICE**  
Springfield, Va. 22151



N72-12221 (NASA-TT-F-14033) TIME-DEPENDENT  
CALCULATION METHOD FOR TRANSONIC NOZZLE  
FLOWS P. Laval (Scientific Translation  
Service) Dec. 1971 37 p

Unclass  
09826

CSCL 20D

G3/12

FAC (NASA CR OR TMX OR AD NUMBER)

NATIONAL AERONAUTICS AND SPACE ADMINISTRATION  
WASHINGTON, D. C. 20546 DECEMBER 1971

# **N O T I C E**

**THIS DOCUMENT HAS BEEN REPRODUCED FROM  
THE BEST COPY FURNISHED US BY THE SPONSORING  
AGENCY. ALTHOUGH IT IS RECOGNIZED THAT CER-  
TAIN PORTIONS ARE ILLEGIBLE, IT IS BEING RE-  
LEASED IN THE INTEREST OF MAKING AVAILABLE  
AS MUCH INFORMATION AS POSSIBLE.**

TIME-DEPENDENT CALCULATION METHOD FOR  
TRANSONIC NOZZLE FLOWS

Pierre Laval

ABSTRACT. A time-dependent method is developed to compute mixed two-dimensional or axisymmetric flow in a nozzle with or without central body. The time-dependent equations of motion are used in conservative form, with transformed spatial independent variables. An explicit second-order accurate difference scheme, similar to a two-step Richtmeyer scheme, is set up with an artificial viscosity term.

Results are presented for an annular nozzle and for five classical axisymmetric nozzles with small throat radius of curvature (the ratio of curvature radius to nozzle radius at the throat varying from 0.8 to 0.1). Excellent agreement is found with experimental data and in particular with experimental results obtained for a conical converging nozzle.

Introduction

/2\*

The problem of mixed flow (subsonic-transonic-supersonic) in a converging-diverging axisymmetric nozzle can be solved theoretically either by analytical or by time-dependent methods.

The solution of this problem is of great practical interest when the ratio of the throat radius of curvature to the nozzle radius at the throat,  $R/h$ , is less than 1, and more especially, when the ratio tends toward zero (truncated cone and convergent).

---

\*Numbers in the margin indicate the pagination in the original foreign text.

Classic analytical methods, such as those of Sauer [1], Oswatitch [2] and Hall [3], are no longer useful when  $R/h$  is of the order of 2.

More recent methods, such as those of Hopkins and Hill [4] and Kliegel and Levine [5] can handle the case of nozzles with smaller radius of curvature ( $R/h < 1$ ). In the first [4], which is an inverse method, the authors used a series expansion in powers of the stream function. In the second [5], solutions are obtained as series expansions with respect to the parameter  $1/1 + R/h$ .

Agreement of these two methods with experiment [6] is satisfactory in the case of a nozzle defined by  $R/h = 0.625$  (at least in the throat), but they do not allow an approach to the case of the convergent truncated cone, since their expansions diverge for  $R/h \leq 1/4$ .

This problem of mixed flow can be studied another way by a time-dependent method. Introduction of time into the flow equations, making them hyperbolic, is known to allow calculation of the entire flow field with the same numerical method, and to give the desired steady flow as the asymptotic limit of a time-dependent flow.

Such a method was first used by Saunders [7] to calculate the transonic flow in a classic axisymmetric nozzle, using an explicit second-order method proposed by Thommen [8], which did not contain a pseudo-viscosity term. However, it has been shown by Burstein [9] that it is necessary to introduce a pseudo-viscosity term to avoid instabilities in a second-order method such as that of [7].

These problems were then treated by Migdal, Klein, and Moretti [10], with a method developed for the problem of a detached shock wave by Moretti and Abbett [11].

In addition, the method of Godunov [12] has been extended to the problem of flow in a classical or annular axisymmetric nozzle by Ivanov [13].

In the present work, a time-dependent method is proposed for calculating the mixed flow in an axisymmetric nozzle with or without a central body.

The flow equations are used in conservative form, the space variables  $(X, Y)$  being regular functions of the variables of the physical plane  $(x, y)$ . These equations are solved numerically by an explicit second-order method which is related to the "two steps in time" method of Richtmyer [14], and which contains a pseudo-viscosity term.

A direct problem is solved by giving a steady-state distribution of the angle  $\theta(X)$  on the lower and upper boundaries of the  $(X, Y)$  net. The nozzles considered are prolonged upstream by a tube of constant cross-section, and the conditions in the inlet are time-dependent.

This method has been applied to calculation of classic axisymmetric nozzles with a small radius of curvature. The results obtained for different values of the parameter  $R/h$  between 0.8 and 0.1 will be presented and compared with experimental results and with those of other analytic or time-dependent methods.

In particular, these results will show that the proposed method allows an approach to the limiting case of the convergent truncated cone. Application of this method to the case of an annular nozzle will also be presented.

We have also established another time-dependent method in which the coordinates  $(X, Y)$  used are images of the streamlines and of their orthogonal trajectories [15], [16]. This method was developed especially to treat a problem of confluence of two flows [17], where use of these coordinates allows the wake boundary to be represented by a line  $Y = \text{constant}$ . For the problem of flow in a nozzle, this second method leads to large difficulties in

calculation, and requires much more computer time than the first (in particular, it requires the calculation of 7 quantities at each point instead of 4).

Since these two methods are similar in principle, and since the numerical results have been obtained with the first method, we will present only that one to shorten the exposition.

### 1. Conservative Equations in Cartesian Coordinates

/3

The equations of motion of a time-dependent compressible planar ( $\epsilon = 0$ ) or axisymmetric ( $\epsilon = 1$ ) flow can be written in the conservative form

$$\frac{dU}{dt} + \frac{dF(U)}{dx} + \frac{dG(U)}{dy} = \epsilon H(U) \quad (1)$$

in Cartesian coordinates  $(x, y)$ .

The vectors  $U$ ,  $F$ ,  $G$  and  $H$  are defined as functions of the usual quantities  $p$  (pressure),  $\rho$  (density),  $V$  (velocity), and  $\theta$  (angle of velocity with x-axis):

$$U = \begin{bmatrix} \rho y^\epsilon \\ \rho V \cos \theta y^\epsilon \\ \rho V \sin \theta y^\epsilon \\ E y^\epsilon \end{bmatrix}, \quad F(U) = \begin{bmatrix} \rho V \cos \theta y^\epsilon \\ (p + \rho V^2 \cos^2 \theta) y^\epsilon \\ \rho V \sin \theta y^\epsilon \\ V \cos \theta (E + p) y^\epsilon \end{bmatrix},$$

$$G(U) = \begin{bmatrix} \rho V \sin \theta y^\epsilon \\ \rho V^2 \cos \theta \sin \theta y^\epsilon \\ (p + \rho V^2 \sin^2 \theta) y^\epsilon \\ V \sin \theta (E + p) y^\epsilon \end{bmatrix}, \quad H(U) = \begin{bmatrix} 0 \\ 0 \\ p \\ 0 \end{bmatrix}.$$

For the case considered here of a perfect gas ( $\gamma = \text{constant}$ ), the total energy is given by:

$$E = \frac{p}{\gamma - 1} + \frac{1}{2} \rho V^2.$$

## 2. Change of Spatial Variables

Flows in axisymmetric nozzles composed of a convergent-divergent channel will be calculated. The nozzles to be considered are classic nozzles, or may have a central body (annular). Let  $y = y_s(x)$  and  $y = y_l(x)$  be the equations of the meridians of the upper and lower walls in the more general case of an annular nozzle (Figure 1, b).

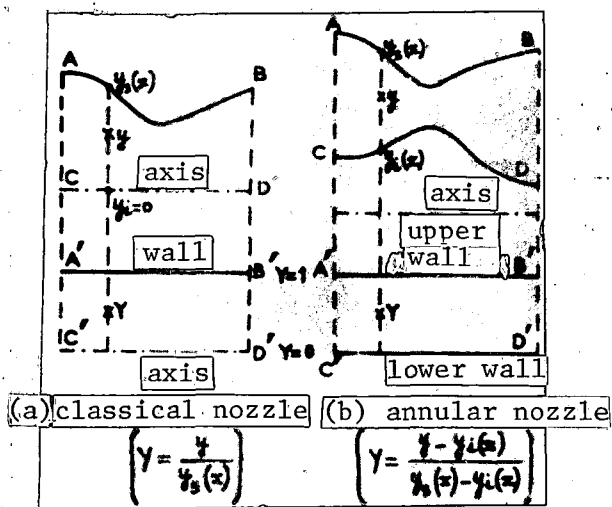


Figure 1

NOT REPRODUCIBLE

In particular, we have studied classic nozzles with very small radius of curvature at the geometric throat ( $0.1 \leq R/h < 0.5$ ), for which it is also necessary to introduce a change of axial variable to expand the region of the geometric throat where changes in the quantities characterizing the flow are very rapid (Figure 2).

To simplify numerical solution, the following change of variables is first carried out:

$$y \rightarrow \eta = \frac{y - y_l(x)}{y_s(x) - y_l(x)}, \quad (2)$$

in order to use a rectangular spatial domain.

The lower (C,D) and upper (A,B) boundaries are then represented by  $\eta = 0$  and  $\eta = 1$  in the transformed plane (Figure 1, a and b).

For this, we have used the following change of variable:

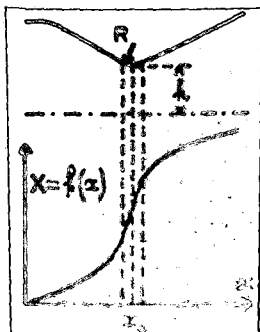


Figure 2. Expansion for  
 $0.1 \leq R/h < 0.5$ .

$$x \rightarrow X = f(x) = \frac{f_1(x) + e^{\frac{1}{2}(x-x_0)} f_2(x)}{1 + e^{\frac{1}{2}(x-x_0)}} \quad (3)$$

with

$$\bar{x} = \frac{x - x_0}{x_0}, \quad f_1(x) = x_0 \left( \frac{1}{2} \bar{x} + k_1 \bar{x}^2 \right) \\ \text{and } f_2(x) = x_0 \left( 2 \bar{x} + k_2 \bar{x}^2 \right),$$

where  $x_0$  is the abscissa of the cross-section of the geometric throat.

The quantities  $k$ ,  $k_1$ , and  $k_2$  are functions of the expansion parameter

$$p_0 = \left( \frac{dy}{dx} \right)_{x_0} = f'(x_0) \\ k = \frac{(2p_0 - 3/2)(8p_0 - 7)}{3p_0 - 5/4}, \quad k_1 = \frac{p_0 - 5/4}{8p_0 - 7} \\ k_2 = \frac{15/4 - 5p_0}{8p_0 - 7}.$$

For nozzles with  $R/h \geq 0.5$ , it is not necessary to use the expansion function. One simply sets  $X = x$ .

### 3. Equations in the New System of Spatial Variables

The new space variables  $(X, Y)$  defined by relations (2) and (3) are non-singular functions of the variables in the physical plane,  $(x, y)$ , so it is known that the equations of motion can be obtained in conservative form in the new system of independent variables  $(X, Y, t)$ . This is shown in [18] and [19], for example.

The system of Equations (1) is thus replaced by the system:

$$\frac{\partial \bar{U}}{\partial t} + \frac{\partial \bar{F}}{\partial x} + \frac{\partial \bar{G}}{\partial y} = \bar{H}, \quad (4)$$

which represents the equations of continuity, of momentum, and of energy in the new variables.

The new vectors  $\bar{U}$ ,  $\bar{F}$ ,  $\bar{G}$  and  $\bar{H}$  are thus defined:

$$\begin{aligned} \bar{U} &= U \cdot x(x), \\ \bar{F} &= F \cdot x(x) \cdot f'(x), \\ \bar{G} &= G \cdot F(y, x) \cdot x'(x) \cdot Y, \\ \bar{H} &= x(x) \left( F \frac{f''(x)}{f'(x)} + \varepsilon H \right), \end{aligned}$$

as functions of

- the original vectors  $U$ ,  $F$ ,  $G$  and  $H$ ;
- quantities related to the nozzle geometry, such as:

$$\begin{aligned} x(x) &= y_2(x) - y_1(x), \quad y_1'(x) = t_{g1} \theta_1(x), \\ x'(x) &= t_{g2} \theta_2(x) - t_{g1} \theta_1(x), \end{aligned}$$

- quantities related to the dilatation function, such as:

$$f'(x) = \frac{dx}{dx} \quad \text{et} \quad f''(x) = \frac{d^2x}{dx^2}$$

Since it is impossible to confuse the vectors of systems (1) and (4), we shall hereafter write the vectors of system (4) without bars.

The components of the vectors  $F$ ,  $G$  and  $H$  are given as functions of the 4 components of the vector  $U$ :

$$\begin{cases} U_1 = \rho y^E x, & U_2 = \rho V \cos \theta y^E x, \\ U_3 = \rho V \sin \theta y^E x & \text{et} & U_4 = E y^E x, \end{cases} \quad (5)$$

by the following relations:

$$\begin{aligned}
 F_1 &= U_2 f', \quad F_2 = \left( p y^E x + \frac{U_2^2}{U_1} \right) f', \\
 F_3 &= \frac{U_2 U_3}{U_1} f', \quad F_4 = \left( U_4 + p y^E x \right) \frac{U_2}{U_1} f', \\
 G_1 &= \frac{1}{x} \left\{ U_3 - U_2 (y_i' + x' y) \right\}, \\
 G_2 &= \frac{1}{x} \left\{ \frac{U_2 U_3}{U_1} - \left( p y^E x + \frac{U_2^2}{U_1} \right) (y_i' + x' y) \right\}, \\
 G_3 &= \frac{1}{x} \left\{ p y^E x + \frac{U_2^2}{U_1} - \frac{U_2 U_3}{U_1} (y_i' + x' y) \right\}, \\
 G_4 &= \frac{1}{x} \left\{ U_4 + p y^E x \right\} \left\{ \frac{U_2}{U_1} - \frac{U_2}{U_1} (y_i' + x' y) \right\}, \\
 H_1 &= \frac{U_2 f''}{f'}, \quad H_2 = \left( p y^E x + \frac{U_2^2}{U_1} \right) \frac{f''}{f'}, \\
 H_3 &= \frac{U_2 U_3}{U_1} \frac{f''}{f'} + \varepsilon \cdot p x, \\
 H_4 &= \left( U_4 + p y^E x \right) \frac{U_2}{U_1} \frac{f''}{f'}.
 \end{aligned} \tag{6}$$

The usual quantities  $p(x, y, t)$ ,  $\rho(x, y, t)$ ,  $V(x, y, t)$  and  $\theta(x, y, t)$  /5  
are expressed as functions of the 4 components of the vector  $\underline{U}(X, Y, t)$  by:

$$\begin{aligned}
 p &= \frac{(x-1)}{y^E x} \left\{ U_4 - \frac{1}{2} \frac{U_2^2 + U_3^2}{U_1} \right\}, \quad (7.1) \\
 \rho &= \frac{U_2}{y^E x}, \quad (7.2) \\
 V &= \frac{\sqrt{U_2^2 + U_3^2}}{U_1}, \quad (7.3) \\
 \theta &= \text{Arctg} \left( U_3 / U_2 \right). \quad (7.4)
 \end{aligned} \tag{7}$$

#### 4. Method of Finite Differences

For numerical solution of the system (4), we have constructed an explicit second-order method, related to a "two-steps-in-time" method of Richtmyer [14].

A rectangular net is defined in the X, Y plane by use of the lines with coordinates  $X_j$  ( $j = 0, 2, 4, \dots, j_{\max}$ ) and  $Y_l$  ( $l = 0, 2, 4, \dots, l_{\max}$ ).

The four components of the vector  $U_{j,l}$  are to be determined at the points of the net  $(X_j, Y_l)$  with  $j = 0, 2, 4, \dots, j_{\max}$  and  $l = 0, 2, 4, \dots, l_{\max}$ . As these quantities are known in the whole X, Y plane at time  $t^n$ , their values are calculated for time  $t^{n+2}$  using two steps in time:

a. First step in time ( $t^n \rightarrow t^{n+1}$ )

$$U_{j,l}^{n+1} = \frac{1}{4} (U_{j+1,l}^n + U_{j-1,l}^n + U_{j,l+1}^n + U_{j,l-1}^n) - \Delta t \left( \frac{F_{j+1,l}^n - F_{j-1,l}^n}{2 \Delta X} + \frac{G_{j,l+1}^n - G_{j,l-1}^n}{2 \Delta Y} \right) + \frac{1}{4} \Delta t (H_{j+1,l}^n + H_{j-1,l}^n + H_{j,l+1}^n + H_{j,l-1}^n)$$

(8)

b. Second step in time ( $t^{n+1} \rightarrow t^{n+2}$ )

$$U_{j,l}^{n+2} = U_{j,l}^{n+1} + \Delta t H_{j,l}^{n+1} + Q_{j,l}^{n+1} - \Delta t \left( \frac{F_{j+1,l}^{n+1} - F_{j-1,l}^{n+1}}{\Delta X} + \frac{G_{j,l+1}^{n+1} - G_{j,l-1}^{n+1}}{\Delta Y} \right)$$

(9)

The components of the vectors

$$F_{j,l}^{n+2} = F_{j,l}^{n+1} (U_{j,l}^{n+1}, t_{j,l}^{n+1})$$

(Equations continued on next page)

$$\begin{aligned} G_{j,l}^{an} &= G_{j,l}^{an}(U_{j,l}^{an}, \gamma_l, z_j, (\delta/\epsilon)_j, (z')_j), \\ H_{j,l}^{an} &= H_{j,l}^{an}(U_{j,l}^{an}, (\delta/\epsilon)_j, \gamma_{j,l}), \end{aligned}$$

are determined through relations (6).

In the second member of (9), we have introduced a pseudo-viscosity term:

$$Q = \chi \frac{\Delta t}{\Delta x} \{ \delta_x (q_x \delta_x U) + \delta_y (q_y \delta_y U) \}, \quad (10)$$

which is of the same type as that defined by Burstein [9].

It is known [9], [14] that a pseudo-viscosity term must be used in a second-order method, even if shock waves are not involved in the flow problem, in order to avoid the nonlinear instabilities inherent in such a method.

The operators  $\delta_x$  and  $\delta_y$  are the differential operators in the X and Y directions. The matrices  $q_x$  and  $q_y$  must be chosen so that they give the desired dissipative effects when the vector  $U$  varies rapidly between two neighboring points, and so that they are negligible when the variation is small. We have adopted the definition of these matrices given in [19]:

$$\begin{aligned} (q_x)_{j,l} &= |u_{j+1,l} - u_{j-1,l}| I, \\ (q_y)_{j,l} &= |v_{j,l+1} - v_{j,l-1}| I, \end{aligned} \quad (11)$$

where  $u$  and  $v$  are the velocity components and  $I$  is the unity matrix.

/6

The parameter  $\chi$  will be defined by relation (13).

The study of the stability of the method proposed in Equations (8) and (9) is given in the appendix. This study, carried out for planar flow ( $\epsilon = 0$ ), leads to the criterion for stability:

$$\frac{\Delta t}{\Delta x} < \frac{\sqrt{\left(\frac{\Delta x}{\Delta t}\right)^2 + 1} - \frac{Y}{\Delta t}}{2|v|_{\max}}, \quad (12)$$

where  $|v|_{\max} = (|V| + c)$  for cartesian coordinates, and a relatively complicated expression for the (X, Y) coordinates used (Equation A.6).

This criterion seems to indicate that it is sufficient to choose the parameter  $\Delta$  of Equation (10) to be equal to a constant of the order of unity, so that the ratio  $\Delta t/\Delta x$  will not be too small. Preliminary numerical tests on a classic nozzle (6.1) have shown that in fact such a choice leads to numerical instabilities in the axial region of the flow, and we have thus been led to define this parameter as a function of Y:

$$\Delta = \Delta_{\max} Y, \quad (13)$$

where  $\Delta_{\max}$  is the value of  $\Delta$  on the wall, a constant of the order of unity. This definition assures stability of all the calculations carried out on classic nozzles (6.1, 2, 3). The definition of  $\Delta$  is different for an annular nozzle, and will be given in Section 6.4.

## 5. Initial and Boundary Conditions

The direct problem is solved by giving a steady-state distribution of the angle  $\theta$  on the upper ( $Y = 1$ ) and lower ( $Y = 0$ ) boundaries:

- for  $Y = 1$ :  $\theta = \theta_s(X)$ , the angle of the meridian of the upper wall;
- for  $Y = 0$ :  $\theta = \theta_i(X)$ , the angle of the meridian of the central body,  
or  $\theta = 0$ , along the axis.

### 5.1 Initial Conditions

Initial values of the flow over the whole  $X, Y$  plane are found by using the law of flow through sections. The angle  $\theta$  is calculated at each section  $X = \text{constant}$  by a linear law:

$$\theta = Y\theta_1(X) + (1-Y)\theta_2(X).$$

The values of the 4 components of the vector  $\vec{U}$ , given by the relations (5), are thus determined at each point of the  $X, Y$  net at the initial time  $t^{n_0}$ .

### 5.2 Boundary Conditions

The flow is next calculated at time  $t^{n_0} + \Delta t$ , using method (8), then at time  $t^{n_0} + 2 \Delta t$ , using method (9), and so on. This allows use at each step of a five-point method<sup>(1)</sup>, and thus calculation of the net  $(X, Y)$  in the whole rectangle interior to  $A'B'C'D'$  (Figure 3). This net must be complete by conditions on the four boundaries:

- a. Upper boundary AB [ $Y = 1, 0 \leq X \leq X_{\max}, \theta = \theta_s(X)$ ]

The three components  $U_1, U_2, U_4$  of the vector  $\vec{U}$  are calculated by parabolic extrapolation at each section  $X = \text{constant}$ . This gives  $U_3 = U_2 + \theta_s(X)$ .

- b. Lower boundary CD ( $Y = 0, 0 \leq X \leq X_{\max}$ )

— This boundary is the nozzle axis ( $\theta = 0$ ):

(1)

Except for the pseudo-viscosity term, which requires special treatment for the points on the contour of the rectangle  $A'B'C'D'$  (Figure 3).

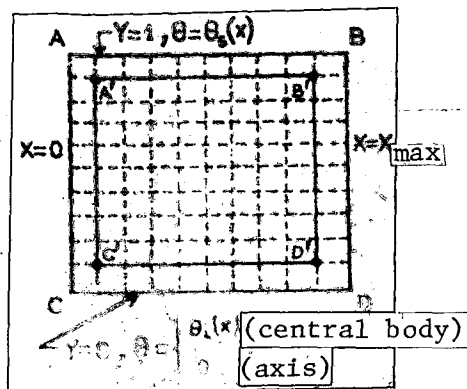


Figure 3

In this case, the symmetry properties of the flow are used in calculating the quantities by parabolic interpolation at each section  $X = \text{constant}$ . In the planar case ( $\epsilon = 0$ ), the interpolation is made for the three components  $U_1$ ,  $U_2$ , and  $U_4$ , while  $U_3 = 0$ . For axial symmetry ( $\epsilon = 1$ ), where  $U_1 = U_2 = U_3 = U_4 = 0$ , the interpolation is made for  $p$ ,  $\rho$ , and  $V$ .

— This boundary is the lower wall

$$[\theta = \theta_1(X)]:$$

The three components  $U_1$ ,  $U_2$  and  $U_4$  are calculated by parabolic extrapolation at each section  $X = \text{constant}$ . This gives  $U_3 = U_1, U_2, U_4$ .

c. Upstream Boundary AC ( $X = 0, 0 < Y < 1$ )

Calculation of upstream conditions is based on the conservation of mass flow by writing that the mass flow  $\mathcal{D}^* = \pi \int_0^1 U_1 dy$  in the inlet section at time  $t + \Delta t$  is equal to the mass flow  $\mathcal{D}^* = \pi \int_0^1 U_1^* dy$  calculated in the geometric throat at time  $t$ .

This method has been used by Saunders [7], with the addition of requiring the upstream conditions to be uniform in  $Y$  (one-dimensional flow), which means that an outlet section must be taken sufficiently upstream in the inlet tube. This increases the number of points in the net considerably, and also the computational time.

To avoid these problems, nonuniform conditions in  $Y$  are imposed in section AC at the downstream end of the tube (Figure 4):

17

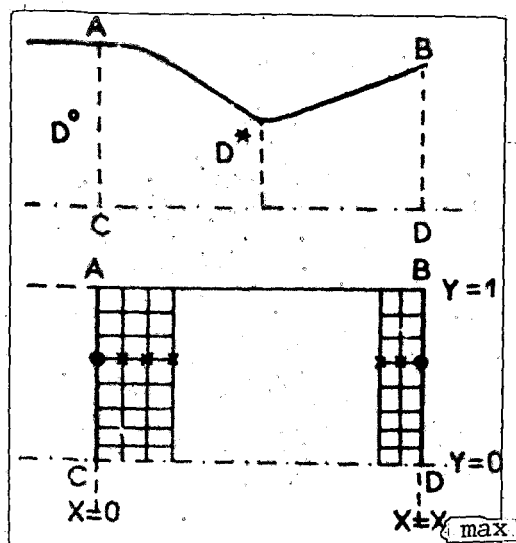


Figure 4

— The four components of the vector  $\vec{U}(0, Y, t)$  are calculated by parabolic extrapolation.

— The value of the component  $U_2(0, Y, t)$  is corrected by consideration of the conservation of mass flow.

d. Downstream boundary BD  
 $(X = X_{\max}, 0 \leq Y \leq 1)$

The quantities are simply calculated by linear extrapolation (Figure 4).

## 6. Results

The results obtained with an IBM 360/50 program are presented and compared with experimental results or with those obtained by other methods.

They concern different classic axisymmetric nozzles for which the parameter  $R/h$  has values of 0.1 - 0.25 - 0.5 - 0.625, 0.8, and one annular nozzle.

In all these applications, the ratio of specific heats  $\gamma$  is taken to be 1.4.

### 6.1 Axisymmetric Nozzle with Small Throat Radius of Curvature ( $R/h = 0.625$ )

This is a nozzle with circular longitudinal section at the throat ( $R/h = 0.625$ ), composed of a  $45^\circ$  convergent and a  $15^\circ$  divergent section (Figure 5).

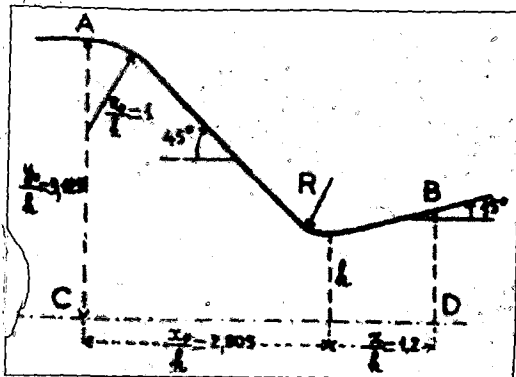


Figure 5. Axisymmetric nozzle ( $R/h = 0.625$ ).

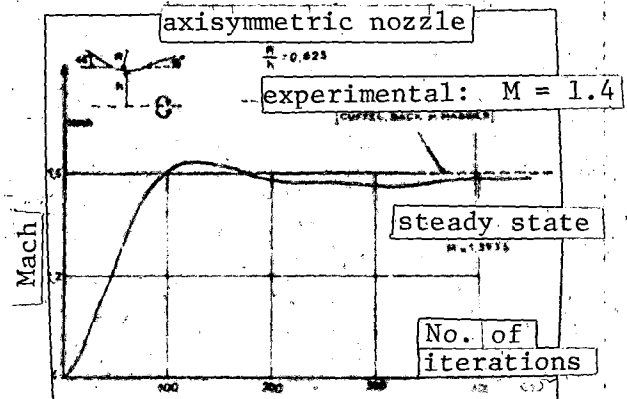


Figure 6. Change of Mach number with time. Point on the wall at the geometric throat.

A detailed experimental study of this nozzle was made by Cuffel, Back, and Massier [6]. It was also studied analytically by Kliegel and Levine [5], and numerically by Prozan [20], using the method of Saunders [7], and by Midgal, Klein, and Moretti [10].

The results presented have been obtained with a 61 by 21 point net in  $(X, Y)$ , without using the expansion function (i.e., with  $X = x$ ). The ratios  $\overline{\Delta t}/\overline{\Delta X}$  and  $\overline{\Delta t}/\overline{\Delta Y}$  are of the order of  $1/17$  and  $1/12$ , respectively, with  $\overline{\Delta X} = \Delta X/h$  and  $\overline{\Delta t} = c_* \Delta t/h$ , where the index  $(*)$  refers to the sonic state. The value chosen for the ratio  $\overline{\Delta t}/\overline{\Delta X}$  is a little smaller than that given by the criterion for stability obtained for plane flow (Equations 12 and A.5). The constant  $\square_{\max}$  appearing in the pseudo-viscosity term (Equation 13) is equal to 1.5 (calculations made with  $\square_{\max} = 1$  or 2 give practically the same asymptotic state).

Figure 6 and 7 show the change in Mach number with time at a point on the wall of the geometric throat and at a point on the throat axis until the steady state is achieved. For these two points, the value of the Mach number remains constant within the accuracy of the method ( $\overline{\Delta t}^2 \sim 2 \times 10^{-5}$ ) from the

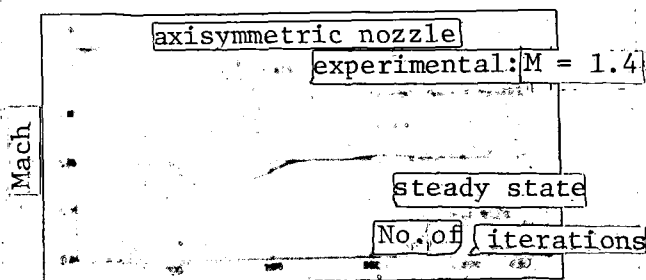


Figure 7. Change of Mach number with time. Point on the axis at the geometric throat.

250<sup>th</sup> to the 280<sup>th</sup> iteration:  $M_{wall} = 1.3820$  and  $M_{axis} = 0.80045$ . The steady state is considered established in the geometric throat when the value of the mass flow there becomes constant (to about  $\Delta t^2$ ), which occurs at the 398<sup>th</sup> iteration (Table 1). The corresponding values of the Mach number are 1.3935 (Figure 6) and 0.824 (Figure 7), respectively, and may be compared to the experimental results of Cuffel, Back, and Massier [6]:  $M_{wall} = 1.4$  and  $M_{axis} = 0.8$ .

The asymptotic value obtained for the mass flow coefficient  $C_D$  in the geometric throat is shown in Table 1, where  $N$  is the number of time iterations. This value is also compared with the values obtained by other methods.

In [5], the value of the mass flow coefficient is obtained by use of the approximate formula

$$C_D = \frac{1}{\left(1 + \frac{R}{h}\right)^{\frac{\gamma}{\gamma-1}}} \left( \frac{1}{1 + \frac{R}{h}} \right)^{\frac{\gamma}{\gamma-1}} \left( \frac{1}{1 + \frac{R}{h}} \right)^{\frac{\gamma}{\gamma-1}} \quad (14)$$

which depends only on  $1/1 + R/h$  and  $\gamma$ , but is independent of the angle of the convergent section. The corresponding value,  $C_D = 0.982$ , thus has only a qualitative nature.

Figure 8 shows the iso-Mach lines obtained (for  $0.6 \leq M \leq 1.6$ ). The distribution of Mach number along the axis is compared with that given by Cuffel, Back, and Massier [6] (Figure 9). This comparison is very satisfactory out to

TABLE 1. VALUE OF THE MASS FLOW COEFFICIENT  $C_D$

$R/h$	$C_D$	
392	0,9849023	
393	0,9850019	
394	0,9850981	MISSEL and LEVINE [7]
395	0,9851984	MISSEL, BACK & MASSIER [6]
396	0,9852966	(Saunders method [7])
397	0,9853979	present method
398	0,9854974	

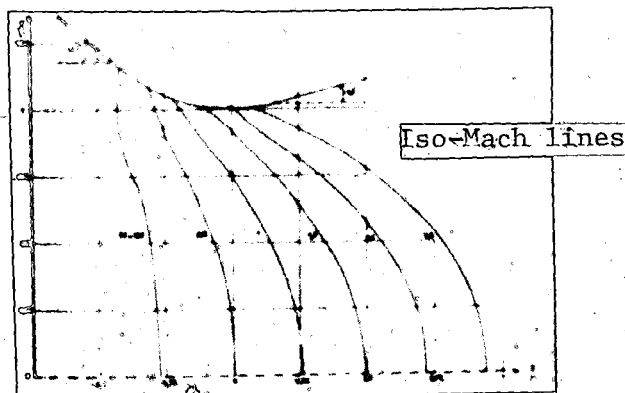


Figure 8. Axisymmetric nozzle  $R/h = 0.625$ .

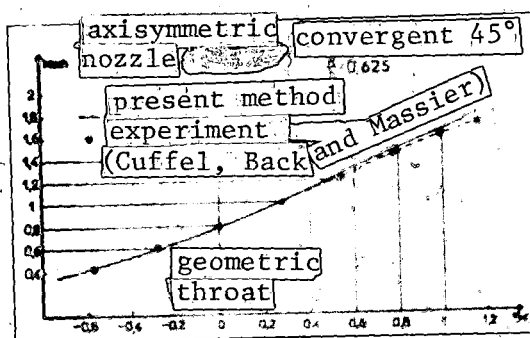


Figure 9. Change of Mach number on the axis.

a value of the Mach number of the order of 1.2<sup>(2)</sup>. In general, comparison of the results obtained for the distribution of Mach number over the whole flow field with experimental results [6] is very satisfactory.

## 6.2 Axisymmetric Nozzle with Very Small Throat Radius of Curvature ( $R/h = 0.1$ )

This is a nozzle with circular longitudinal section at the throat ( $R/h = 0.1$ ), composed of a 20° convergent and a 20° divergent section (Figure 10).

<sup>(2)</sup> It should be noted, however, that the values of [6], taken from the published paper, are not very precise, and that consequently this comparison is less significant than comparisons made with points on the wall and on the axis in the geometric throat (Figures 6 and 7), for which the authors [6] stated definitely the value obtained for the Mach number.

The difficulty in this calculation, which requires use of the expansion function  $X = f(x)$  defined by relation (3), lies in the choice of the parameter  $p_0 = \left(\frac{dX}{dx}\right)_{x_0} = f'(x_0)$  fixing the expansion of the region of the geometric throat where the quantities characterizing the flow vary extremely rapidly (Table 3). Too small a value of  $p_0$  ( $p_0 < 3$ ) gives insufficient expansion; too large a value ( $p_0 > 4$ ) creates numerical instabilities outside the region of rapid transition, due to too-large values of the ratio  $\frac{dX}{dx}$ . This appears in the second term of Equation (4).

The results presented were obtained with  $p_0 = 3.4$ . The net contained 68 by 23 points (X, Y). The ratios  $\overline{\Delta t}/\overline{\Delta X}$  and  $\overline{\Delta t}/\overline{\Delta Y}$  are of the order of 1/16 and 1/15, respectively. The constant  $\overline{\Delta t}_{\max}$  of Equation (13) is equal to 1.15.

The changes of the Mach number as a function of time at a point on the wall of the geometric throat and at the axis at the throat are shown in Figure 11. For these two points, the asymptotic value of the Mach number is practically attained at the 270<sup>th</sup> iteration. Table 2, which gives the mass flow coefficient  $C_D$  in the throat as a function of N, the number of iterations, shows that the steady state can be considered to have been attained at the 278<sup>th</sup> iteration in this section, when the corresponding value  $C_D = 0.968988$  is obtained with an accuracy greater than that of the method ( $\overline{\Delta t}^2 \sim 10^{-5}$ ), and then varies extremely little out to the final iteration (N = 375).

The geometry of the iso-Mach lines (obtained from the 375<sup>th</sup> iteration) is given by Figure 12, which shows in particular that the variation of Mach number is very rapid on the wall, since the sonic point is situated on the rectilinear portion, very near the junction with the circular portion, while the Mach number is 1.821 on the wall of the geometric throat. This variation is shown clearly in Table 3, which gives the value of the Mach number as a function of  $\theta_{\text{wall}}$  (the angle of the meridian of the wall), of  $x/h$ , and of  $X/h$  (x is the cartesian coordinate, and X is the expanded coordinate).

/10

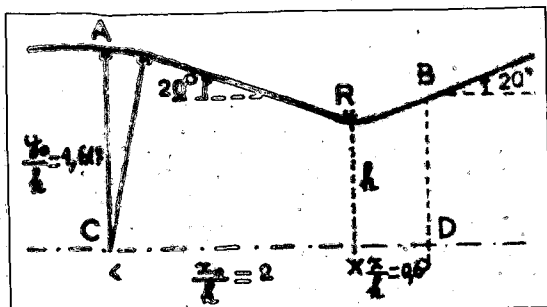


Figure 10. Axisymmetric nozzle ( $R/h = 0.1$ ).

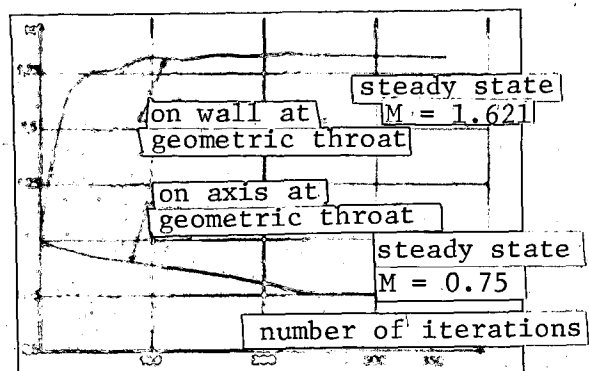


Figure 11. Change of Mach number with time. Axisymmetric nozzle.  $20^\circ$  convergent section  $R/h = 0.1$

TABLE 2. MASS FLOW COEFFICIENT,  $20^\circ$  CONVERGENT SECTION.  $R/h = 0.1$ .

$\gamma$	$C_D$
275	0,9690063
276	0,9689981
277	0,9689925
278	0,9689889
279	0,9689884
280	0,9689896
300	0,969543
325	0,970453
350	0,969428
375	0,969079

TABLE 3. MACH NUMBER ON THE WALL.

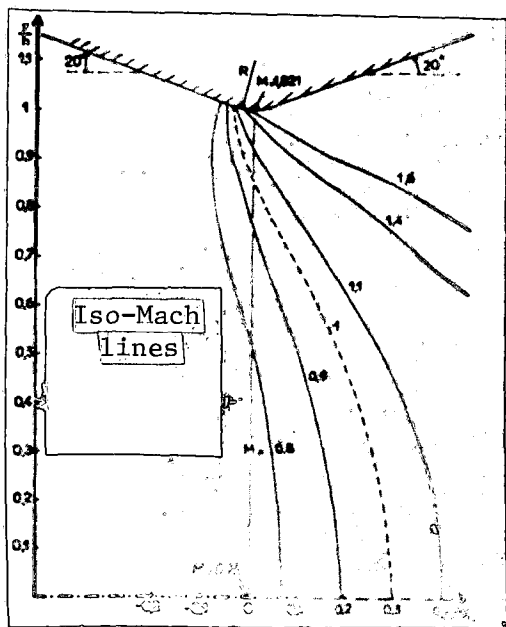


Figure 12. Axisymmetric nozzle with very small throat radius of curvature ( $R/h = 0.1$ )

	$x/h$	$\theta$	Mach	$x/h$
linear portion	-0,0484	$-20^\circ$	0,949	0,1429
	-0,0790	$-20^\circ$	1	0,1353
	-0,0948	$-20^\circ$		0,1163
junction	-0,0281	$-16^\circ 31'$	1,250	0,0952
	-0,0140	$-6^\circ 06'$	1,596	0,0476
	0	0	1,821	0
circular portion				

### 6.3 Axisymmetric Nozzle with a 20° Convergent Section and Varying R/h Ratios

To show that the present method can handle the case of a truncated cone convergent section, the preceding study has been completed by carrying out calculations for a nozzle composed of a 20° convergent and a 20° divergent section for three other values of the parameter R/h: 0.25 - 0.5 - 0.8. The case for R/h = 0.25 was treated by taking the expansion parameter  $p_0 = 2.5$ , while in the other two calculations (R/h = 0.5 and 0.8) no expansion function was used ( $X = x$ ).

The results are compared with experimental results of O.N.E.R.A. [21] for a 20° truncated cone convergent section for an ideal gas ( $\gamma = 1.4$ ).

Figure 13 shows the position of the sonic line as a function of R/h. The agreement with the experimental results is very satisfactory.

Figure 14 shows the mass flow coefficient in the geometric throat as a function of R/h. By extrapolation of the results obtained for the four values of R/h (0.1 - 0.25 - 0.5 - 0.8), a mass flow coefficient of 0.968 is obtained for R/h = 0. The relatively large difference (3/1000) between this result and the experimental result of  $C_D = 0.971$  is due in part to difficulties in the experimental measurements in the region of the angle apex, which result in a certain amount of uncertainty in the determination of the test line (peak or characteristic line) along which the mass flow is calculated. It is for this reason that experimental points for the sonic line are not given for values of the ordinate y/h greater than 0.8 (Figure 13).

Comparison between results of the present method for the mass flow coefficient in a nozzle with 20° convergent section and the results obtained with the approximate Formula (14) of Kliegel and Levine [5], independent of the angle of the convergent section, is made in Table 4, which shows clearly that the fourth order expansion  $O(\frac{1}{h^4})$  is no longer significant when R/h = 0.25.

/11

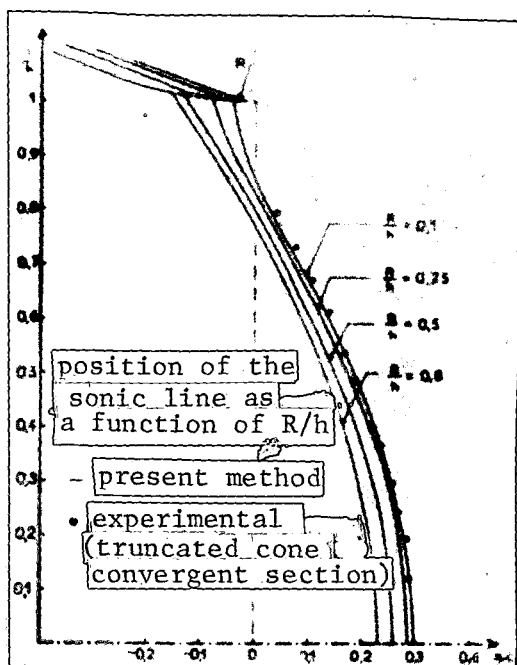


Figure 13. Axisymmetric nozzle.  
20° convergent section.

TABLE 4. MASS FLOW COEFFICIENT AS A  
FUNCTION OF  $R/h$

$R/h$	present method*	Kliegel 3rd order	Kliegel 4th order**
0.8	0.962212	0.989462	0.966112
0.5	0.977318	0.984012	0.977066
0.25	0.971380	0.975573	0.961169
0.1	0.968988	0.966974	0.942956
0	(0.968)	0.958542	0.923377

\* 20° convergent section

\*\* Development independent of the  
convergent section angle

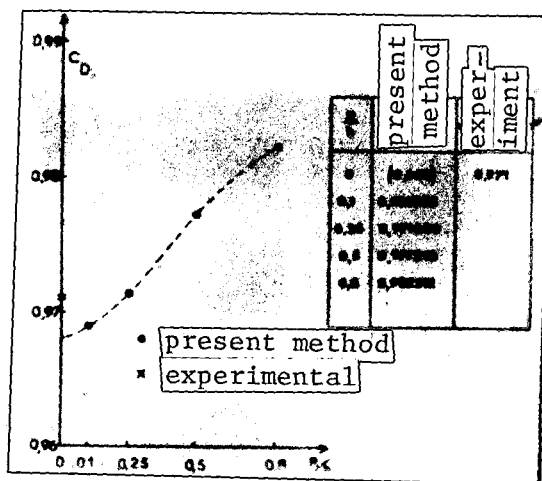


Figure 14. Axisymmetric nozzle with  
20° convergent section. Variation  
of the mass flow coefficient with  
 $R/h$

#### 6.4 Annular nozzle<sup>(3)</sup>

The example chosen has been  
treated earlier by Ivanov [13].

The upper wall of this nozzle is  
a cylinder of radius  $y_s = 5$ . The longi-  
tudinal section of the lower wall is  
composed of the straight line  $y_0 = 1$ ,  
and of three circular arcs with radii  
4, 2.43, and 8.5, respectively  
(Figure 15).

<sup>(3)</sup> Computations for this nozzle were carried out by Mlle. Mortire of the  
O.N.E.R.A. Computer Center.

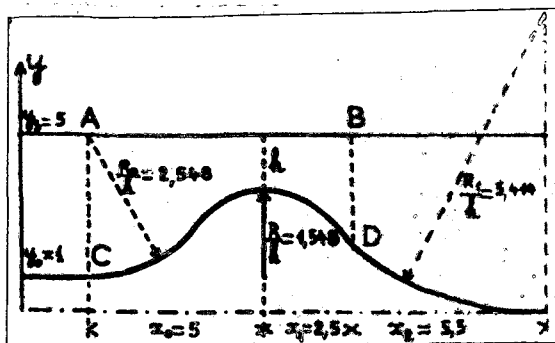


Figure 15. Annular nozzle.

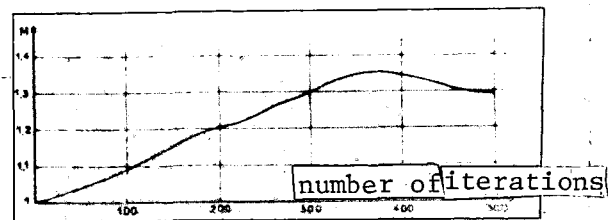


Figure 16. Annular nozzle. Change of Mach number with time. Point on the lower wall in the geometric throat

Calculation of such a nozzle differs from that of a classic nozzle mainly in the choice of the parameter  $\gamma$  in the pseudo-viscosity term. Numerical tests have led to the following definition:

$$X = X_0(1 - \gamma)$$

The results presented have been obtained by taking  $\gamma$ , the value of  $\gamma$  on the lower wall, equal to 0.25.

It must be pointed out that establishment of the steady-state regime is much slower for this annular nozzle than for the classical nozzles treated previously; this is shown in Figure 16, which gives the change in Mach number as a function of time at the point on the lower wall at the geometric throat. It can be seen that the Mach number has not attained its asymptotic value even after 500 iterations, which corresponds to computing time of more than three hours on the IBM 360/50 [for a net of 75 by 17 points (X, Y)].

These difficulties in obtaining steady state were also encountered by Ivanov [13], who emphasized the slowness of convergence in the slightly subsonic region of the convergent section.

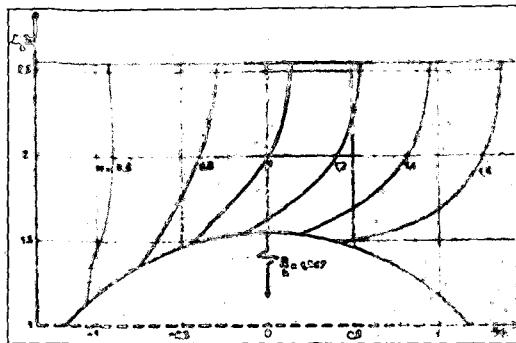


Figure 17. Annular nozzle.  
Iso-Mach lines.

Figure 17 shows the geometry of the iso-Mach lines in this nozzle. These lines are slightly more inclined than the iso-Mach lines obtained by Ivanov. This difference can be accounted for in two ways:

- The lines have been obtained by the present method out to the 500<sup>th</sup> iteration, while the steady state was not finally established. (This would require prohibitive computer time.)
- The calculations of Ivanov were carried out with a net of wider spacing.

### Conclusion

The results obtained, and particularly their excellent agreement with the experimental results, show that the problem of transonic flow in an axisymmetric nozzle can be solved quite satisfactorily by a second-order difference method containing a pseudo-viscosity term.

The method proposed contains the following special points:

- a) Conditions in the inlet section of the nozzle are time-dependent, the mass flow in this section being equal at any time step to the mass flow calculated in the section of the geometric throat (5.2 c).
- b) The parameter  $\lambda$  of the pseudo-viscosity term is defined as a function of the spatial variable  $Y$  (relations 13 and 15).
- c) Use of an expansion function  $X = f(x)$  (relation 3) allows this method to be extended to nozzles with very small radius of curvature ( $R/h = 0.1$ );

and to approach the case of a truncated cone convergent section, as is shown by comparison with experiment (6.3).

- d) This method can also be applied to the problem of annular nozzles (6.4) (a problem also treated by Ivanov [13] with the aid of the method of Godunov [12]).

In common with all second-order, conservative methods, the present one requires a relatively dense net, and consequently, relatively long computer time. The different applications to classic nozzles which have been presented, required on the order of two hours on the IBM 360/50. The steady state was obtained for a nozzle with very small radius of curvature ( $T/h \approx 0.1$ ) after 135 minutes of computation for a net of 68 by 23 points (X, Y). Use of a relatively dense net does, however, allow the steady flow to be determined with good accuracy. If one takes into consideration the fact that the length of computation can be reduced by taking initial values not as far away from the steady state as those given by the law of sections, it can be seen that this method is a tool for numerical computation which is not only precise, but also relatively rapid.

#### REFERENCES

/13

1. Sauer, R. General Characteristics of the Flow Through Nozzles at Near Critical Speeds. TM-1147, N.A.C.A., June 1947.
2. Oswatitch, K. and W. Rothstein. Flow Pattern in a Converging-Diverging Nozzle. TM-1215, N.A.C.A., March 1949.
3. Hall, I.M. Transonic Flow in Two Dimensional and Axially-Symmetric Nozzles. Quarterly Journal of Mechanics and Applied Mathematics, Vol. XV, Part 4, 1962, pp. 487-508.
4. Hopkins, D.F. and D.E. Hill. Effect of Small Radius of Curvature on Transonic Flow in Axisymmetric Nozzles. A.I.A.A. Journal, Vol. 4, No. 8, August 1966, pp. 1337-1343.
5. Kliegel, J.R. and J.N. Levine. Transonic Flow in Small Throat Radius of Curvature Nozzles. A.I.A.A. Journal, Vol. 7, No. 7, July 1969, pp. 1375-1378.
6. Cuffel, R.F., L.H. Back and P.F. Massier. Transonic Flowfield in a Supersonic Nozzle with Small Throat Radius of Curvature. A.I.A.A. Journal, Vol. 7, No. 7, July 1969, pp. 1364-1366.
7. Saunders, L.M. Numerical Solution of the Flow Field in the Throat Region of a Nozzle. BSVD-P-66-TN-001, August 1966.
8. Thommen, H. Numerical Integration of the Navier-Stokes equations. G.D. CONVAIR ERRAN, August 1965, p. 759.
9. Burstein, S.Z. Finite Difference Calculation for Hydrodynamic Flow Containing Discontinuities. Journal of Computational Physics, Vol. 1, No. 2, November 1966.
10. Migdal, D., K. Klein and G. Moretti. Time Dependent Calculations for Transonic Nozzle Flow. A.I.A.A. Journal, Vol. 7, No. 2, February 1969, pp. 372-373.
11. Moretti, G and M. Abbett. A Time-Dependent Computational Method for Blunt Body Flows. A.I.A.A. Journal, Vol. 4, No. 12, December 1966, p. 2136.

12. Gudonov, S.K., A.V. Zabrodine and G.P. Prokopov. Finite-Difference Method for Solution of Time-Dependent Problems. Application to the Calculation of Flow with a Detached Shock Wave. *Journal de Mathématique et de Physique Mathématique*, 1961, pp. 1020-1050.
13. Ivanov, M. and A.H. Kraiko. Numerical Solution of the Problem of Mixed Flow in a Nozzle (Direct Problem). *Journal de la Mécanique des liquides et des gaz*, No. 5, 1969, pp. 77-83.
14. Richtmyer, R.D. and K.W. Morton. Difference Methods for Initial Value Problems Tracts in Mathematics. Second Edition, No. 4, Interscience Publishers Inc., New York, 1967.
15. Carriere, P. Method for Numerical Calculation of a Steady-State Compressible Flow  $(x, y)$  as the Asymptotic Limit of a Time-Dependent Flow  $(x, y, t)$ . *C.R. Acad. Sci.*, Vol. 266A, April 1968, pp. 1015-1018.
16. Laval, P. Construction of an Explicit and Precise Second-Order Difference Scheme for the Calculation of Planar or Axisymmetric Compressible Flow. *C.R. Acad. Sci.*, Vol. 267A, November 1968, pp. 754-756.
17. Laval, P. Construction of an Explicit and Precise Second-Order Finite-Difference Scheme of the LAX-WENDROFF Type, with Two Steps in Time. Application to the Calculation of the Equilibrium Configuration of Two Compressible Co-Axial Axisymmetric Flows. Unpublished O.N.E.R.A. Document, September 1968.
18. Anderson, J.L., S. Preiser and E.L. Rubin. Conservation Form of the Equations of Hydrodynamics in Curvilinear Coordinate Systems. *Journal of Computational Physics*, Vol. 2, No. 3, February 1968.
19. Lapidus, A. A Detached Shock Calculation by Second Order Finite Differences. *Journal of Computational Physics*, Vol. 2, No. 2, November 1967.
20. Prozan, R.J. Cited in a reference by R.F. Cuffel, L.H. Back and P.F. Massier [6]. Private Communication, Lockheed Missiles and Space Co., Huntsville, Ala., 1968.
21. Solognac, J.L. Experimental Study of Conical Convergents. To be published.

## Appendix A Section 4

### Stability of the Method

The stability of the proposed method is studied for the case of planar flow ( $\epsilon = 0$ ) in a nozzle without a central body, with  $R/h \geq 0.5$ . The change of spatial variables is then defined by  $\xi = x/h, \eta = y/h$  (no expansion function).

Under these conditions, the vector  $H$  appearing in the second member of system (4) is zero.

The linearization hypotheses are as follows:

The matrices  $A$  and  $B$ , jacobians of the vectors  $F$  and  $G$ , as well as the scalar matrices  $Q_x$  and  $Q_y$  defined by Equation (11), are supposed to be locally constant.

In that case, one may set

$$F = AU, G = BU$$

$$Q = X \frac{\Delta t}{2\Delta x} \{ q_x \delta_x^2 U + q_y \delta_y^2 U \}$$

and may carry out a Fourier analysis by setting  $U_n = U_0 e^{i(n\Delta x + 2\pi n\eta)}$  where  $U_0$  is a constant vector for each value of  $n$ .

The amplification matrix  $M(U_0 = MU_0)$  of the system (8) and (9) is written (taking  $\Delta x = \Delta y$ )

$$M(\beta, \eta, \Delta t) = \left\{ 1 - X \frac{\Delta t}{2\Delta x} (q_x \sin^2 \beta + q_y \sin^2 \eta) \right\} I$$

$$- i (\cos \beta + \cos \eta) \frac{\Delta t}{\Delta x} C - 2 \left( \frac{\Delta t}{\Delta x} C \right)^2$$

(A.1)

where

$$C = A \sin \theta + B \sin \eta,$$

$$\xi = k_x \Delta x, \quad \eta = k_y \Delta y.$$

Since the direct calculation of the eigenvalues of the matrix  $C$  is too complicated, the system of equations will be considered in Eulerian form, as was done in [14], in which the matrices  $A'$  and  $B'$  are simpler than the matrices  $A$  and  $B$  in the linearized system of (4):

$$A' = \begin{pmatrix} V \cos \theta & \rho & 0 & 0 \\ 0 & V \cos \theta & 0 & 1/\rho \\ 0 & 0 & V \cos \theta & 0 \\ 0 & \rho c^2 & 0 & V \cos \theta \end{pmatrix}$$

$$B' = \begin{pmatrix} b & -\rho c^2 & 0 & 0 \\ 0 & b & 0 & -\gamma g_s / \rho \\ 0 & 0 & b & 1/\rho \\ 0 & -\rho c^2 / \gamma g_s & \rho c^2 & b \end{pmatrix}$$

where

$$b = V(\sin \theta \cos \theta / \gamma g_s)$$

By similarity, one can go from this Eulerian system to the linearized system (4). The eigenvalues of the amplification matrix  $M$  are invariant under similarity, so matrix  $C$  of (A.1) can be replaced by the matrix  $C' = A' \sin \theta + B' \sin \eta$  for which the eigenvalues can be calculated without difficulty:

$$A' = \begin{pmatrix} V \cos \theta & \rho & 0 & 0 \\ 0 & V \cos \theta & 0 & 1/\rho \\ 0 & 0 & V \cos \theta & 0 \\ 0 & \rho c^2 & 0 & V \cos \theta \end{pmatrix}$$

(A.3)

with:

$$\begin{aligned} u' &= V(m \cos \theta + n \sin \theta), \\ m &= \cos \theta_1 - \gamma \frac{y_2}{y_3} \sin \theta_1, \\ n &= \frac{\sin \theta_1}{y_3}, \end{aligned}$$

where the angle  $\theta_1$  is defined by:

$$\tan \theta_1 = \frac{\gamma \frac{y_2}{y_3} \sin \theta_1}{\cos \theta_1 - \gamma \frac{y_2}{y_3} \sin \theta_1}$$

The eigenvalues of M are expressed as functions of the eigenvalues of C' by the relation:

$$\lambda^2 - \left( \gamma_1 \frac{y_2}{y_3} + \gamma_2 \frac{y_1}{y_3} \right) \lambda + \left( \gamma_1 \frac{y_2}{y_3} \gamma_2 \frac{y_1}{y_3} \right) = 0$$

(A.4)

Note that  $\max$   $\lambda$   $\max$ , where  $|\lambda|_{\max}$  is the maximum eigenvalue of C', and since  $\gamma_1 < \frac{y_1}{y_3}$  and  $\gamma_2 < \frac{y_2}{y_3}$ , the method is stable in the Neumann sense if

$$\frac{\Delta t}{\Delta x} < \frac{1}{\max \left( \gamma_1 \frac{y_2}{y_3} + \gamma_2 \frac{y_1}{y_3} \right)}$$

(A.5)

where  $|\nu|_{\max}$  allows for increasing K:

$$K = \begin{cases} \sqrt{(\gamma_1 + c)^2 + \frac{1}{y_3^2} (\gamma_2 + c - \gamma_3 (1 + c))^2} & \text{for } \gamma_1 = \gamma_2 < 0 \\ \sqrt{(\gamma_1 + c)^2 + \frac{1}{y_3^2} (\gamma_2 + c)^2} & \text{for } \gamma_1 = \gamma_2 > 0 \end{cases}$$

(A.6)

This criterion, established for planar flow, can be used only qualitatively for applications to axisymmetric flow. The value of this stability study is that it confirms the necessity of introducing a stabilizing pseudo-viscosity term. Thus, relation (A.4) shows that if the pseudo-viscosity term is not considered ( $\chi=0$ ), eigenvalues  $|\mu|$  are strictly equal to 1 when the eigenvalues  $|\lambda|$  of  $C'$  are zero, i.e., when  $u'=0$  (in particular  $V'=0$ ) and  $\mu' = \pm c \sqrt{a^2 + b^2}$  from Equation (A.3), so the method is not stable for these particular values. Since the scalar matrices  $q_x$  and  $q_y$  are chosen positive (Equation 10), the method with viscosity will always be stable when criterion (A.5) is satisfied.

Translated for National Aeronautics and Space Administration under Contract No. NASw 2035, by SCITRAN, P.O. Box 5456, Santa Barbara, California, 93108.

## ABSTRACT

### INTRODUCTION

The calculation of mixed flow in a converging-diverging axisymmetric nozzle is of great practical interest in the case when the ratio of throat radius of curvature to the nozzle radius at the throat  $R/r_0$  is small. This problem can be solved either by analytical methods (HOPKINS and HILL 1966, KLIEGEL and LEVINE 1969) or by numerical time-dependent methods (SAUNDERS 1966, MIGDAL, KLEIN and MORETTI 1969, IVANOV 1969).

In the present work, a time dependent method is used to calculate mixed two-dimensional or axisymmetric flows in a nozzle with or without central body. The equations of motion are written in terms of transformed spatial variables and solved by means of an explicit second-order scheme. The results will show that the method proposed here allows to approach the limiting case of the conical converging nozzle.

A different time-dependent method was also set up in which the independent variables are the images of the streamlines and of their orthogonal trajectories (P. CARRIERE 1968, P. LAVAL 1968). However, for the problem considered here, this method proved to be much more complicated and lead to much longer computing times than the first one, and it will not be presented here. A number of details which cannot be given here will be available in a more extensive paper to be published soon (P. LAVAL 1970).

### I - GENERAL EQUATIONS

In the general case of axisymmetric or of two-dimensional nozzle with central body, let  $x$  and  $y$  represent the non-dimensional axial and radial or transversal coordinates, and let  $y = y_u(x)$  and  $y = y_l(x)$  be the equations of the upper and lower walls. The reference length is such that  $y_u(x_0) = y_l(x_0) = 1$  at the throat. The transformed coordinates are defined by the equations :

$$(1) \quad y \rightarrow Y = \frac{y - y_l(x)}{y_u(x) - y_l(x)},$$

$$(2) \quad x \rightarrow X = f(x) = \frac{f_1(x) + \epsilon^{A_1(x-1)} f_2(x)}{1 + \epsilon^{A_1(x-1)}},$$

where  $\bar{x} = \frac{x}{x_0}$ ,  $x_0$  is the throat abscissa,  $f_1(x) = x_0(1 + A_1 \bar{x})$ ,  $f_2(x) = x_0(1 + A_1 \bar{x}^2)$ .

The following conditions are imposed at the throat :  $f(x_0) = x_0$ ,  $f'(x_0) = 0$ . The parameters  $A_1$ ,  $A_2$  and  $A_3$  can thus be expressed as functions of the only parameter  $\epsilon = f'(x_0)$ .

The transformation from  $y$  to  $Y$  is made in order to obtain a rectangular domain (Fig. 1). The transformed axial variable  $X$  is used in the case of classical nozzles with very small throat radius of curvature ( $0.1 \leq \frac{R}{r_0} < 0.5$ ). It allows to stretch the throat region where large gradients occur (Fig. 2). When  $\frac{R}{r_0} \geq 0.5$ , the stretching is not used ( $X = x$ ).

The coordinates transformation being regular, it is possible (ANDERSON, LAPIDUS) to write the time-dependent equations of motion in conservative form in the new variables  $X, Y, t$  :

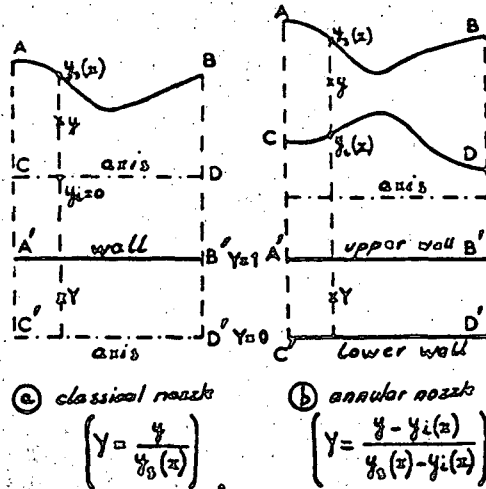


FIGURE 1

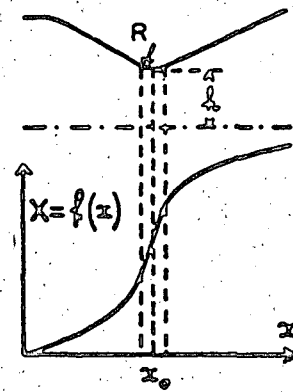


FIGURE 2 :

Stretching for  $0.4 \leq \frac{h}{L} \leq 0.5$

$$(3) \quad \frac{\partial U}{\partial t} + \frac{\partial F}{\partial x} + \frac{\partial G}{\partial y} = H.$$

The components of the vector  $U$  are :

$$(4) \quad U_1 = \rho y^2 \Omega, \quad U_2 = \rho V \cos \theta y^2 \Omega, \quad U_3 = \rho V \sin \theta y^2 \Omega, \quad U_4 = E y^2 \Omega,$$

where  $\Omega(x) = y_0(x) - y_1(x)$ ,  $\theta$  is the angle of the velocity vector with the  $x$ -axis,  $E = \Phi/(\gamma-1) + 1/2 \rho V^2$  is total energy for a perfect gas. The parameter  $\Omega$  is equal to 0 for plane flow and to 1 for axisymmetric flow.

The components of the vectors  $F$ ,  $G$  and  $H$  are given in terms of the components of  $U$  and of geometrical variables such that  $y'_i = \Omega_i \Omega_i(x)$ ,  $x'_i = \Omega_i \Omega_i(x) - \Omega_i \Omega_i(x)$ ,  $f'_i(x)$  and  $f''_i(x)$  :

$$(5) \quad F = F(U, f'), \quad G = G(U, \gamma, x, y'_i, x'), \quad H = H(U, f''/f', y).$$

## II - FINITE-DIFFERENCE SCHEME

A rectangular net of points is defined in the  $X, Y$  plane with the coordinate lines  $X_j$  ( $j=0, 1, 2, \dots, J$ ) and  $Y_l$  ( $l=0, 1, 2, \dots, L$ ). Let  $U_{j,l}^n$  be the value of  $U$  at the point  $X_j = j \Delta X$ ,  $Y_l = l \Delta Y$  and at time  $t^n = n \Delta t$ , with  $n=0, 1, 2, \dots, N$ .

We use the following explicit, second order scheme :

$$(6) \quad U_{j,l}^{n+1} = \frac{1}{4} (U_{j+1,l}^n + U_{j-1,l}^n + U_{j,l+1}^n + U_{j,l-1}^n) - \Delta t \left( \frac{F_{j+1,l}^n - F_{j-1,l}^n}{2 \Delta X} + \frac{G_{j,l+1}^n - G_{j,l-1}^n}{2 \Delta Y} \right) + \frac{1}{4} \Delta t (H_{j+1,l}^n + H_{j-1,l}^n + H_{j,l+1}^n + H_{j,l-1}^n).$$

$$(7) \quad U_{j,l}^{n+1} = U_{j,l}^n - \Delta t \left( \frac{F_{j+1,l}^{n+1} - F_{j-1,l}^{n+1}}{\Delta X} + \frac{G_{j,l+1}^{n+1} - G_{j,l-1}^{n+1}}{\Delta Y} \right) + 2 \Delta t H_{j,l}^{n+1} + Q_{j,l}^{n+1}.$$

The vectors  $F_{j,l}^{n+1}$ ,  $G_{j,l}^{n+1}$  and  $H_{j,l}^{n+1}$  are determined through equations (5).

A pseudo-viscosity term is added to the right-hand side of (7) :

$$(8) \quad Q = \chi \frac{\Delta t}{\Delta x} \left( \delta_x (q_x \delta_x U) + \delta_y (q_y \delta_y U) \right),$$

which is of the type defined by BURSTEIN.

One knows (BURSTEIN, RICHTMYER) that it is necessary to use pseudo-viscosity term in a second-order scheme in order to avoid non-linear instabilities. The matrices  $q_x$  and  $q_y$  are given by the expressions (LAPIDUS) :

$$(9) \quad (q_x)_{j,l} = |u_{j+1,l} - u_{j-1,l}| I, \quad (q_y)_{j,l} = |v_{j,l+1} - v_{j,l-1}| I,$$

where  $u$  and  $v$  are the velocity components and  $I$  is the unit matrix.

The study of the stability was made for plane flows and the results are given in (P. LAVAL, 1970).

For classical nozzles, preliminary numerical calculations have lead to define the parameter  $\chi$  which appears in (8) as a linear function of  $y$  :

$$(10) \quad \chi = \chi_w y,$$

where  $\chi_w$ , the value of  $\chi$  at the wall, is of order unity.

### III - INITIAL AND BOUNDARY CONDITIONS

For a given nozzle, the value of  $\theta$  is known on the upper ( $y=1$ ) and lower ( $y=0$ ) boundaries (Fig. 3).

The initial values of  $p$ ,  $\rho$  and  $V$  are obtained from the one-dimensional approximation, the angle  $\theta$  being calculated by a linear interpolation :  $\theta = \gamma \theta_1(x) + (1-\gamma) \theta_2(x)$

For the flow values at the upper and lower boundaries, a parabolic extrapolation is used, taking into account the relation  $U_D = U_0 \cos^2(\theta)$ . When the lower boundary is the nozzle axis, the flow symmetry is taken care of by a parabolic interpolation.

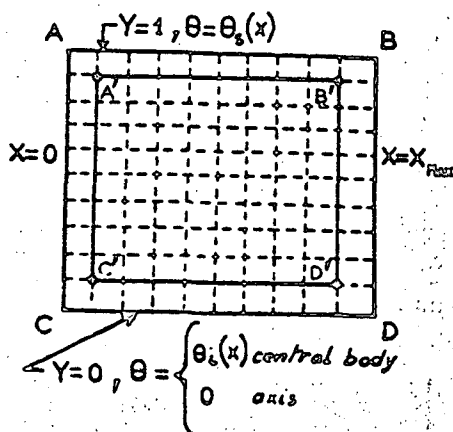


FIGURE 3

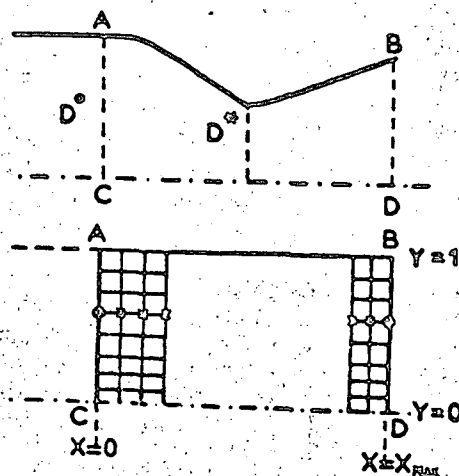


FIGURE 4

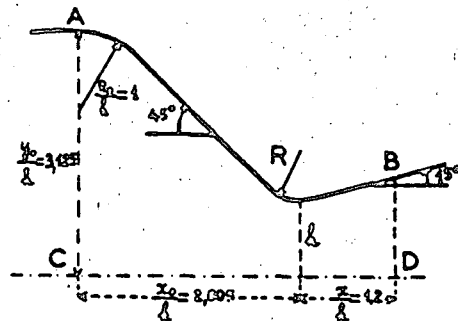
Time-dependent conditions are imposed at the entrance section AC by calculating the components of  $\vec{U}$  by a parabolic extrapolation. The component  $U_x$  is then corrected by writing that the mass flow rate  $\dot{D}^0$  through the entrance section at time  $t + \Delta t$  is equal to the mass flow rate through the throat section at time  $t$  (Fig. 4).

At the exit section BD, values are extrapolated linearly (Fig. 4).

#### IV - RESULTS

Calculations have been carried out on a 360/50 IBM computer, for  $\gamma = 1.4$ .

##### IV.1 - Axisymmetric nozzle with small throat radius of curvature ( $R/r_n = 0.625$ )



This nozzle which is made of a 45° convergent and a 15° divergent (Fig. 5) has been studied by various authors (CUFFEL, KLIEGEL, PROZAN, MIGDAL).

The results have been obtained with a net of  $61 \times 21$  points  $(x, y)$  and with  $X_{max} = 1.5$ , the stretching of the axial coordinate being not used.

Steady state is considered to be obtained at the throat when the mass flow rate change at each iteration becomes smaller than  $\Delta \dot{D}^0 = 10^{-6}$ . This occurs after 398 iterations (Table I). The corresponding values of the Mach number are 1.3935 at the wall (Fig. 6) and 0.8 on the axis (Fig. 7). These values can be compared with CUFFEL's experimental values :  $M_{wall} = 1.4$  and  $M_{axis} = 0.8$ .

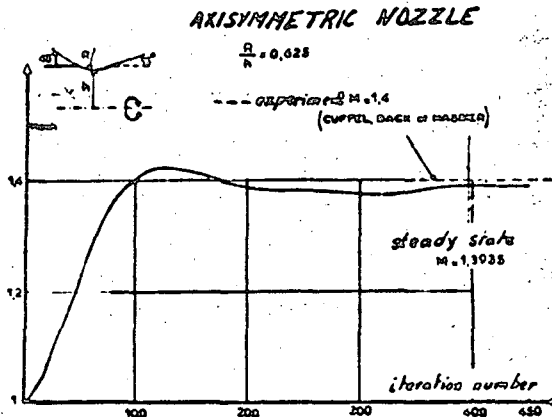


FIGURE 6 : Throat section Mach number on wall vs time.

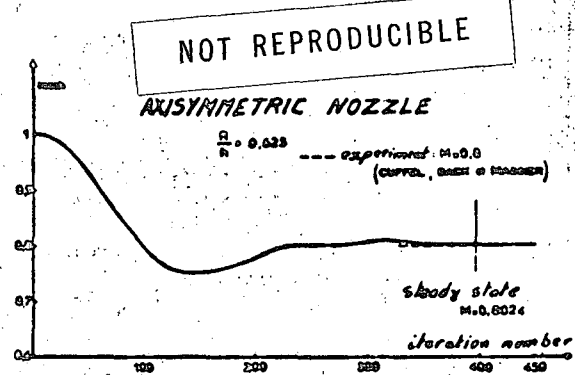


FIGURE 7 : Throat section Mach number on axis vs time.

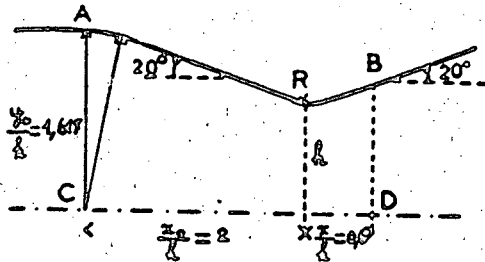
TABLE I - Discharge coefficient  $C_D$

N	$C_D$
392	0.9849025
393	0.9850113
394	0.9850981
395	0.9851634
396	0.9852066
397	0.9852279
398	0.9852274

KLIEGEL & LEVINE	0.982
CUFFEL, BACK & MASSIER	0.985
PROZAN (SAUNDERS method)	0.990
Present method	0.985227

The values of the discharge coefficient  $C_D$  calculated at the throat section for the last seven iterations are given in Table I, where N is the iteration number. The asymptotic value is compared with values obtained by other methods.

IV.2 - Axisymmetric nozzle with very small throat radius of curvature ( $R/L = 0.1$ )



Convergent and divergent angles are both equal to  $20^\circ$  (Fig. 8).

Stretching of the axial coordinate is used with  $\phi_0 = 3.4$ . A net of  $68 \times 23$  points  $(X, Y)$  is used, with  $X_{max} = 1.15$ . Table II gives the discharge coefficient at the throat. One sees that after 278 iterations  $C_D$  changes by less than  $10^{-6}$  and one can consider that the asymptotic value of  $C_D$  is 0.968988.

FIGURE 8 : Axisymmetric nozzle ( $R/L_{20,0}$ )  $C_D$  is 0.968988.

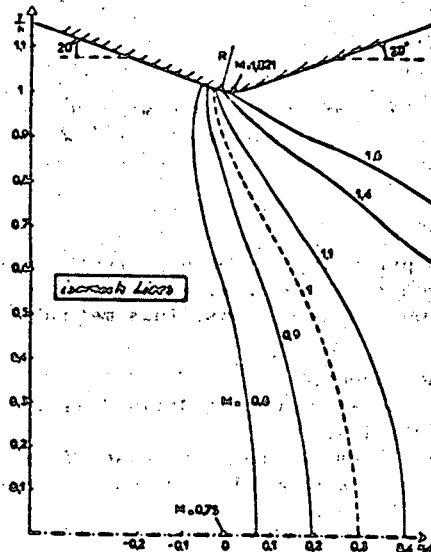


TABLE II - Discharge coefficient

N	$C_D$
275	0.9690063
276	0.9689981
277	0.9689923
278	0.9689889
279	0.9689884
280	0.9689896
300	0.969543
325	0.970453
350	0.969428
375	0.969079

FIGURE 9 : Axisymmetric nozzle with very small throat radius of curvature ( $R/L = 0.1$ )

From Figure 9 it can be seen that large variations of Mach number occur, particularly at the wall, on the rectilinear part of which the sonic point is located, very close to the circular part, whereas the Mach number is equal to 1.831 at the throat section.

IV.3 - Axisymmetric nozzle with a  $20^\circ$  convergent and varying  $R/L$  ratios

To study the approach to the limiting case of a conical converging nozzle, calculations have been made for three values of  $R/L$  : 0.25 - 0.5 and 0.8, besides the value  $R/L = 0.1$  (IV.2). The results will be compared with experiments carried out at O.N.E.R.A. (SOLIGNAC) for a  $20^\circ$  conical converging nozzle.

Excellent agreement is found between theory and experiment concerning the location of the sonic line (Fig. 10). Extrapolating the numerical results relative to the 4 values of  $R/L$ , one obtains  $C_D = 0.968$  for  $R/L = 0$  (Fig. 11). The difference between this value and the experimental result  $C_D = 0.971$  can be explained partly by the difficulty of the measurements in the neighbourhood of the angular point.

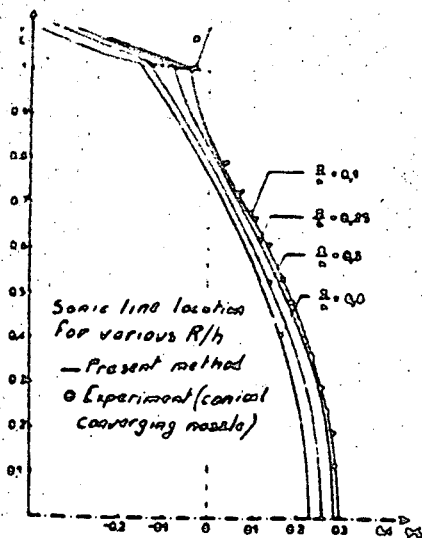


FIGURE 10 : Axisymmetric nozzle  
20° convergent.

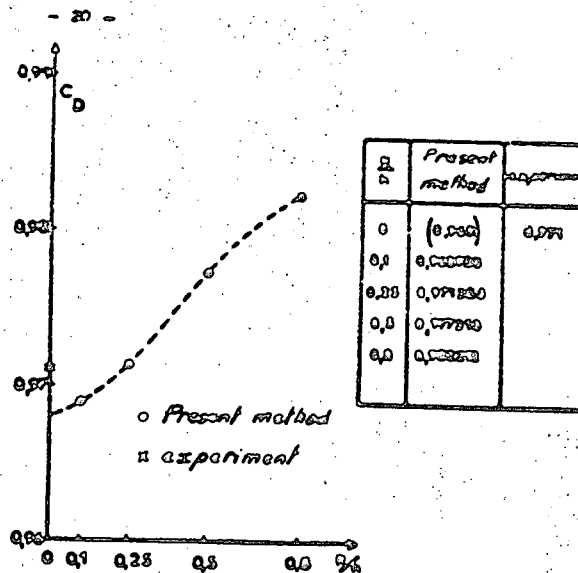


FIGURE 11 : Axisymmetric nozzle with 20°  
convergent. Discharge coefficient vs.  $R/L$ .

### CONCLUSION

The calculations which have been presented, and particularly the excellent agreement which has been found between experimental and numerical results, show that the proposed method is well suited for calculating transonic nozzle flows. This method presents the following particular features :

- conditions in the entrance section are time-dependent;
- the parameter  $\chi$  which appears in the pseudo-viscosity term is defined as a function of the transformed coordinate  $\gamma$  (equ. 10);
- a stretching of the axial coordinate (equ. 2) allows to treat the case of very small throat radius of curvature and to approach the case of a conical converging nozzle;
- the method is applicable also to annular nozzles (P. LAVAL, 1970).

### REFERENCES

- ANDERSON, J.L., PREISER, S., and RUBIN, E.L., J. of computational phys., **2**, No 2, pp. 279-287 (1968).
- BURSTEIN, S.Z., J. of computational physics, **1**, No 2, pp. 198-222 (1966).
- CARRIERE, P., C.R.Ac.Sc., t. 266 A, pp. 1015-1018 (1968).
- CUFFEL, R.F., BACK, L.H., and MASSIER, P.F., AIAA J., **7**, No 7, pp. 1364-1366 (1969).
- HOPKINS, D.F., and HILL, D.E., AIAA J., **4**, No 8, pp. 1337-1343 (1966).
- IVANOV, M., and KRAIKO, A.H., Mekh. Zhidkosti i gaza (in Russian), No 8, pp. 77-82 (1969).
- KLIEGEL, J.R., and LEVINE, J.N., AIAA J., **7**, No 7, pp. 1375-1378 (1969).
- LAPIDUS, A., J. of computational phys., **2**, No 2, pp. 154-177 (1967).
- LAVAL, P., C.R.Ac.Sc., t. 267 A, pp. 754-756 (1968).
- LAVAL, P., N.T.ONERA, to be published (1970).
- MIGDAL, D., KLEIN, K., and MORETTI, G., AIAA J., **7**, No 2, pp. 372-373 (1969).
- PROZAN, R.J.\*
- RICHTMYER, R.D., and MORTON, K.W., Tracts in Mathematics, second edition, No 4, Interscience publishers (1957).
- SAUNDERS, L.M., BSVD - P 66 - TN - 001 (1966).
- SOLIGNAC, J.L., La Recherche Aéronautique, to be published (1970)

\* Private communication to CUFFEL, R.F., above reference.

NOT REPRODUCIBLE